

RESEARCH

Open Access



# Empirical Equation for Mechanical Properties of Lightweight Concrete Developed Using Bottom Ash Aggregates

Hye-Jin Lee, Sanghee Kim , Hak-Young Kim, Ju-Hyun Mun and Keun-Hyeok Yang

## Abstract

The mechanical properties of lightweight aggregate concrete developed with the use of bottom ash aggregate (LWAC-BA) as a partial or full replacement of lightweight aggregate differ from those of general lightweight concrete made using natural fine and/or coarse aggregates. The mechanical properties of LWAC-BA are difficult to predict using the existing equations proposed by codes or researchers. Therefore, in this study, empirical equations using nonlinear regression analysis are proposed to predict the mechanical properties of lightweight concrete mixed with bottom ash aggregate, based on the collected measured values from other studies (Yang "Development of replacement technology for ready mixed concrete with bottom ash aggregates", 2020; Kim et al. *Appl Sci*, 10: e8016, 2020; *Constr Build Mater* 273: e121998, 2021). The collected data include density, compressive strength, elastic modulus, modulus of rupture, splitting tensile strength, and stress–strain relation of LWAC-BA featuring varying amounts of bottom ash fine aggregate and/or coarse aggregate. The proposed empirical equations for each mechanical characteristic are developed considering the replacement volume of bottom ash fine/coarse aggregates. The mean values of the ratios of the measured to predicted values obtained using the proposed equation range from 1.00 to 1.05, with a standard deviation ranging from 0.002 to 0.013, indicating a reasonably positive agreement.

**Keywords:** lightweight concrete, bottom ash, empirical equation, mechanical properties, stress–strain curve, nonlinear regression analysis

## 1 Introduction

Many researchers continue to struggle to identify new materials for replacing conventional ingredients for concrete mixtures. This is because the natural resources used in concrete are becoming increasingly scarce. In particular, the by-products and waste materials are net positive, with examples such as fly ash, blast-furnace slag, and bottom ash. These materials satisfy the research objectives as they are economical and preserve nature by recycling resources. Among by-products, bottom ash is an incombustible by-product collected from the bottom furnace

of thermal power stations. Many researchers reported that bottom ash aggregate has irregular rough surface and porous structure (Kim et al., 2020, 2021; Lee, 2018; Lee et al., 2021; Nisnevich et al., 1999). Due to its porous structure, bottom ash aggregate has a dry density of about 40–70% compared with normal-weight aggregate, while its moisture content is approximately 5–20%, which represents a factor of 3–13 times higher than that of natural aggregate (Lee et al., 2021). The density of aggregate is an important factor that in turn affects the density and quality of concrete (Lee et al., 2019b). As constituents of bottom ash,  $\text{SiO}_2$  and  $\text{Al}_2\text{O}_3$  account for more than 60% of the total composition,  $\text{Fe}_2\text{O}_3$  accounts for approximately 15%, and  $\text{CaO}$  accounts for about 10%. Bottom ash aggregate was effective at improving the long-term strength and durability of concrete, as insoluble and

\*Correspondence: sanghee0714@kyonggi.ac.kr  
Department of Architectural Engineering, Kyonggi University, Suwon,  
Kyonggi-Do 16227, Republic of Korea  
Journal information:ISSN 1976-0485 / eISSN 2234-1315

stable calcium silicate which was produced by pozzolanic reactivity between the bottom ash aggregate and calcium hydroxide (Kim, 2015).

Kim et al. (2021) conducted an experimental study on the effects of concrete unit weight on the mechanical properties of concrete containing bottom ash and determined that density was an important factor in determining mechanical properties. Kim et al. (2020) also investigated the workability and mechanical properties of concrete produced with bottom ash aggregates in relation to three water-to-cement ratios and the replaced ratio of bottom ash aggregates. The slump was seen to decline regardless of the water-to-cement ratio. Bottom ash coarse aggregates had a relatively larger effect on compressive strength than fine aggregate, and the tensile and shear friction strength rose as the density of concrete increased.

Lee et al. (2019b) investigated the various mechanical properties of LWAC mixed with expanded bottom ash and dredged soil-based artificial lightweight aggregates and novel formulas were proposed to anticipate early-age and long-term strength for that. The research revealed that the density of LWAC mixed with expanded bottom ash and dredged soil-based artificial lightweight aggregates was a key factor for determining compressive strength. To examine the feasibility of applying pre-cast concrete panels, Yang et al. (2019) evaluated the consistency and mechanical properties of LWAC mixed with bottom ash with a pre-formed foam volume ratio of less than or equal to 25%. In concrete mixture, ordinary Portland cement was partially replaced with 50% ground-granulated blast-furnace slag and 20% fly ash, while natural fine and coarse aggregates were fully replaced with bottom ash aggregates. As observed in the results, the splitting tensile strength and modulus of rupture declined as foam volume fraction increased.

Lee et al. (2019a) examined the mechanical properties of lightweight aggregate concrete made with expanded bottom ash and dredge soil granules (LWAC-BS), proposing an equation to predict compressive strength, elastic modulus, tensile strength, shear friction, bond strength and also to determine the relationship between compressive strength and strain. Yang (2019) conducted an experiment to investigate the effect of the water-to-cement ratio ( $W/C$ ) and replacement ratio of bottom ash aggregate on the mechanical properties of LWAC-BA. The value of measured compressive strength ( $f'_{c,meas}$ ) of LWAC-BA increased with lower  $W/C$  and higher density, which was likely a tendency of general LWAC. The value of the elastic modulus divided by the square root of  $f'_{c,meas}$  increased smoothly as the density of LWAC-BA was increased. The value of the splitting tensile strength of LWAC-BA was lower than that of general LWAC, and

the value of the modulus fracture divided by the square root of  $f'_{c,meas}$  of LWAC-BA declined slightly as the density of LWAC-BA increased. The bond strength ( $\tau_b$ ) between LWAC-BA and the reinforcing steel-bar was considered weak, because the value of  $\tau_b$  divided by the square root of  $f'_{c,meas}$  of LWAC-BA was lower than that of LWAC-BS.

As described previously, concrete mixed with partial or full bottom ash aggregate possesses mechanical properties that differ from those of conventional LWAC. Therefore, this study aimed to develop empirical equations for mechanical properties such as density ( $\rho_c$ ), compressive strength ( $f'_c$ ), elastic modulus ( $E_c$ ), stress-strain relationship, splitting tensile strength ( $f_{sp}$ ) modulus of rupture ( $f_r$ ), and bond strength ( $\tau_b$ ) of concrete in consideration of the replacement volume of bottom ash fine and coarse aggregates based on nonlinear regression (NLR) analysis and collected experimental data. The proposed empirical equations were compared with the existing design equations, such as ACI 318, *fib* Model Code (2010) (hereafter MC2010), and Lee et al., (2019a, 2019b).

## 2 Development of Equation

Recently, Yang (2020), Kim et al. (2020), and Kim et al. (2021) conducted experimental studies to investigate how the mechanical properties of LWAC-BA differed when the bottom ash fine and/or coarse aggregates were fully or partially replaced with normal-weight aggregates. In the present study, the data related to LWAC-BA in Yang (2020), Kim et al. (2020), and Kim et al. (2021) were collected. Table 1 presents the LWAC-BA mixtures made with partially or fully replaced bottom ash fine aggregate (BAS) and/or bottom ash coarse aggregate (BAC), where each value is the average of three samples. The main parameters observed during the test were the percentage of replaced BAS content ( $R_{BAS}$ ), the percentage of replaced BAC content ( $R_{BAC}$ ), and the water-to-cement ratio ( $W/C$ ), which ranged from 0.3 to 0.45. For example, an  $R_{BAS}$  value of 25% indicated that BAS was used as one-fourth of the total sand aggregate. In Table 1, average measures of the mechanical properties at 28 days are given for the following: oven-dried density ( $\rho_{c,meas}$ ), compressive strength ( $f'_{c,meas}$ ), splitting tensile strength ( $f_{sp,meas}$ ), elastic modulus ( $E_{c,meas}$ ), and bond strength ( $\tau_{b,meas}$ ). In the case of LWAC-BA, which consisted of concrete mixed with partial or full bottom ash aggregate,  $\rho_{c,meas}$  ranged from 1730 to 2171 kg/m<sup>3</sup>,  $f'_{c,meas}$  ranged from 23.3 to 52.6 MPa,  $f_{sp,meas}$  ranged from 2.34 to 3.95 MPa,  $E_{c,meas}$  ranged from 18.1 to 27.9 MPa,  $f_{r,meas}$  ranged from 3.9 to 6 MPa, and  $t_{b,meas}$  ranged from 4.3 to 7 MPa. Utilizing LWAC-BA mixtures and measured values as given in Table 1, as well as the NLR analysis performed

**Table 1** Summary of LWAC-BA mixtures and test results (Kim et al., 2020, 2021; Yang, 2020).

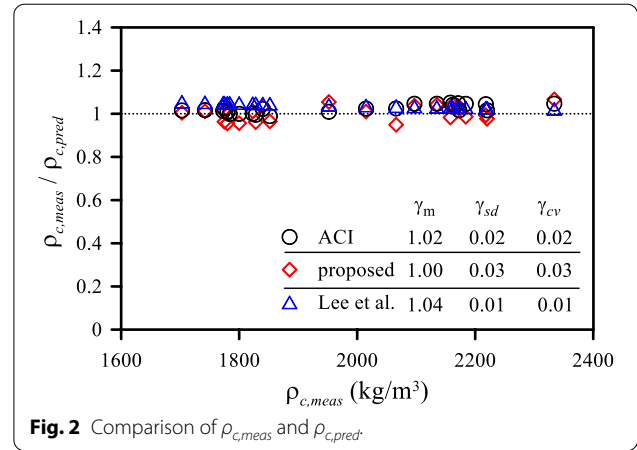
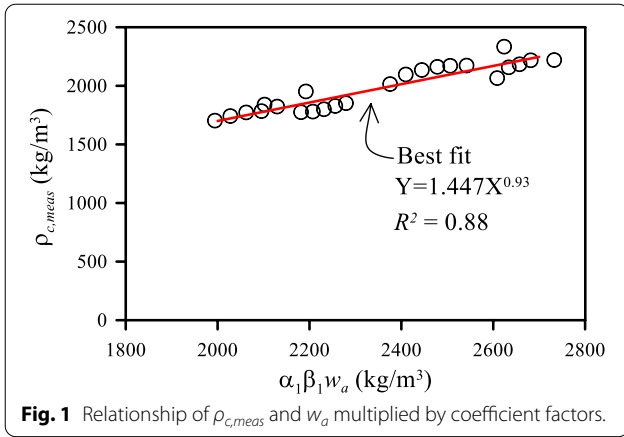
Specimens	W/C	$R_{BAS}$ (%)	$R_{BAC}$ (%)	S/a (%)	Unit volume weight (kg/m <sup>3</sup> )						$A_c$ (%)	$\rho_{c,meas}$ kg/m <sup>3</sup>	$f'_{c,meas}$ MPa	$f_{sp,meas}$ MPa	$f_{r,meas}$ MPa	$E_{c,meas}$ MPa	$\tau_{b,meas}$ MPa
					W	C	$F_s$	BAS	$C_G$	BAC							
L-0-0	0.45	100	100	45	175	389	0	614	0	654	5.5	1703	23.3	2.34	3.93	18,082	4.3
L-25-0	0.45	75	100	45	175	389	189	460	0	654	5	1742	23.8	2.3	4.1	18,685	4.33
L-50-0	0.45	50	100	45	175	389	378	307	0	654	5.2	1773	27	2.35	4.96	19,269	4.75
L-75-0	0.45	25	100	45	175	389	567	153	0	654	5.4	1784	27.7	2.12	4.62	20,197	4.67
L-100-0	0.45	0	100	45	175	389	756	0	0	654	5	1823	27.5	2.96	4.89	21,483	5
L-0-100	0.45	100	0	45	175	389	0	614	932	0	5.2	2015	36.4	3.29	4.97	22,208	5.98
L-25-100	0.45	75	0	45	175	389	189	460	932	0	5.3	2097	41.2	3.47	5.41	25,109	7.1
L-50-100	0.45	50	0	45	175	389	378	307	932	0	5.5	2135	42.9	3.64	5.37	25,291	6.77
L-75-100	0.45	25	0	45	175	389	567	153	932	0	5	2162	40.9	3.68	4.83	24,254	6.21
L-100-100	0.45	0	0	45	175	389	768	0	946	0	4.7	2173	39.2	3.65	4.73	22,223	6.25
M-0-0	0.3	100	100	45	175	583	0	590	0	629	5.8	1775	29.5	3.28	5.39	22,493	5.21
M-25-0	0.3	75	100	45	175	583	182	443	0	629	5.9	1780	28.3	2.37	4.75	20,944	4.77
M-50-0	0.3	50	100	45	175	583	364	295	0	629	5.4	1800	28.8	2.37	4.61	21,827	4.65
M-75-0	0.3	25	100	45	175	583	546	148	0	629	5.5	1828	30.3	2.47	4.75	21,954	4.75
M-100-0	0.3	0	100	45	175	583	728	0	0	629	5	1852	30.6	3.28	5.51	22,058	4.98
M-0-100	0.3	100	0	45	175	583	0	590	896	0	5.4	2066	42.8	3.48	5.81	25,572	5.83
M-25-100	0.3	75	0	45	175	583	182	443	896	0	5.5	2158	42.4	3.74	5.37	25,380	6.62
M-50-100	0.3	50	0	45	175	583	364	295	896	0	4.8	2184	46.3	3.73	6.45	25,699	7.1
M-75-100	0.3	25	0	45	175	583	546	148	896	0	5	2218	48.8	3.89	6.53	26,961	7.34
M-100-100	0.3	0	0	45	175	583	739	0	910	0	4.7	2220	46.1	3.9	6.16	25,410	7.03
H-0-0	0.3	100	100	45	175	583	0	555	0	592	4.8	1840	41.3	3.8	5.55	23,072	4.45
H-100-0	0.3	0	100	45	175	583	684	0	0	592	5	1952	40.7	3.77	4.54	22,316	5.22
H-0-100	0.3	100	0	45	175	583	0	555	843	0	5.2	2171	52.6	3.95	6	27,877	7.03
H-100-100	0.3	0	0	45	175	583	696	0	857	0	5.5	2334	52.1	4.11	6.16	27,419	6.79

$R_{BAS}$  is the percentage of replaced content of BAS (= 100 × BAS's weight to total sand weight);  $R_{BAC}$  is the percentage of replaced content of BAC aggregate (= 100 × BAC's weight to total coarse weight); W/C is the water-to-cement ratio; S/a is the fine aggregate ratio; W is the water volume; C is the cement;  $F_s$  and  $C_G$  are the natural sand and coarse aggregates, respectively; BAS and BAC are the bottom ash fine and coarse aggregate, respectively;  $A_c$  is the air content; and  $\rho_{c,meas}$ ,  $f'_{c,meas}$ ,  $f_{sp,meas}$ ,  $f_{r,meas}$ ,  $E_{c,meas}$  and  $\tau_{b,meas}$  are the measured density, compressive strength, splitting tensile, modulus of rupture, elastic modulus, and bond strength at 28 days, respectively.

by Yang et al. (2014a, 2014b)) and Lee et al. (2019a), new straightforward empirical equations for LWAC-BA were derived in the order of  $\rho_c$ ,  $f'_c$ ,  $E_c$ ,  $\epsilon_0$ , stress–strain,  $f_{sp}$ ,  $f_r$ , and  $\tau_b$ . Due to the internal number of voids of bottom ash aggregate, bottom ash aggregate generally possessed lower crushing strength and stiffness compared with natural aggregate (Sim & Yang, 2011). Its property affects the compressive strength of concrete, and the compressive strength and weight of the unit volume of bottom ash aggregate are generally inversely proportional to each other (Lee et al., 2021). Therefore, the proposed model presented in this study was more simplified by using the weight of the unit volume of bottom ash aggregate and the compressive strength. The presented model evaluated the mean, standard deviation, and coefficient of variation through comparative analysis with experimental results.

### 2.1 Oven-Dried Density

As previously reports by Yang (2020), Kim et al. (2020), Kim et al. (2021), the measured oven-dried density ( $\rho_{c,meas}$ ) of LWAC-BA was affected by W/C,  $R_{BAS}$ , and  $R_{BAC}$ . Therefore, an equation for oven-dried density should be considered with W/C,  $R_{BAS}$ , and  $R_{BAC}$ , and two coefficient factors were to be derived. To determine the weight of the effects of BAC, the volume of natural sand ( $F_s$ ) used was fixed. The weight was then calculated from the relationship between  $R_{BAC}$  and  $\rho_{c,meas}$  to  $w_a$ , where  $w_a$  is the summation of the absolute unit weight of each ingredient. After that, the weight of the effects of W/C was also calculated from the relationship between W/C and the ratio of  $\rho_{c,meas}$  to  $w_a$ . From the weights of the effects of BAC and W/C, the following coefficient factor ( $\alpha_1$ ) pertaining to BAC and W/C was finally derived:



$$\alpha_1 = \left(0.0013 \left(\frac{W}{C}\right) - 0.0009\right) R_{BAC} + \left(-0.3736 \left(\frac{W}{C}\right) + 1.1177\right) \quad (1)$$

By using the same method and procedure, a second coefficient factor ( $\beta_1$ ) regarding BAS and  $W/C$  was also derived:

$$\beta_1 = \left(-0.0011 \left(\frac{W}{C}\right) + 0.0006\right) R_{BAS} + \left(0.3076 \left(\frac{W}{C}\right) + 1.0367\right) \quad (2)$$

Fig. 1 shows the relationship of the measured density ( $\rho_{c,meas}$ ) and the summation of the absolute unit weight of each ingredient ( $w_a$ ) multiplied by the coefficient factors ( $\alpha_1$  and  $\beta_1$ ) for the NLR analysis. By utilizing NLR analysis, the straightforward empirical equation for oven-dried density ( $\rho_c$ ) of LWAC-BA can be expressed as

$$\rho_c = 1.447(\alpha_1\beta_1w_a)^{0.93}, \quad (3)$$

where  $\rho_c$  is the oven-dried density (in  $\text{kg/m}^3$ ) and  $w_a$  is the summation of the absolute unit weight of each ingredient (in kilograms). The correlation coefficient ( $R^2$ ) was 0.88.

Fig. 2 displays a comparison of  $\rho_{c,meas}$  and values of predicted oven-dried density ( $\rho_{c,pred}$ ) obtained by using proposed model, ACI 318 (2019), and Lee et al.'s (2019a) equation. The mean value ( $\gamma_m$ ), standard derivation ( $\gamma_{sd}$ ), and coefficient of variation ( $\gamma_{cv}$ ) of the measured to predicted density obtained by using the proposed equation are 1.00, 0.03, and 0.034, respectively. Meanwhile, the values of  $\gamma_m$  of ACI 318 (2019) and the equation of Lee et al. (2019a) are close to 1, while the values of  $\gamma_{sd}$  and  $\gamma_{cv}$  of ACI 318 (2019) and the equation of Lee et al. (2019a)

are slightly higher than those of the proposed equation. However, all values of  $\gamma_{cv}$  are 0.03 or less. Overall, the accuracy of the proposed model and the others is similar and acceptable.

## 2.2 Compressive Strength

Yang et al. (2014a, 2014b) proposed an equation to predict the compressive strength ( $f'_c$ ) of LWAC. The model was formulated with  $\rho_c$  and  $C/W$  (cement-to-water ratio) as the primary parameters, and Lee et al. (2019a) modified the equation so that LWAC-BS would fit. The relationship among compressive strength ( $f'_c$ ), oven-dried density, and  $C/W$  of LWAC-BA can be expressed as

$$\frac{f'_c}{f'_0} = 1.544 \left[ \alpha_2 \beta_2 \left(\frac{\rho_c}{\rho_0}\right)^{0.8} \left(\frac{C}{W}\right)^{1.47} \right]^{0.44}, \quad (4)$$

where

$$\alpha_2 = \left(-0.015 \left(\frac{W}{C}\right) + 0.002\right) R_{BAC} + \left(0.8 \left(\frac{W}{C}\right) + 0.8\right), \quad (5)$$

$$\beta_2 = \left(0.007 \left(\frac{W}{C}\right) - 0.0039\right) R_{BAS} + \left(2.935 \left(\frac{W}{C}\right) + 0.283\right). \quad (6)$$

In aforementioned equations,  $f'_c$  is the compressive strength of LWAC-BA (in MPa);  $f'_0$  is the reference compressive strength (= 10 MPa);  $R_{BAS}$  is the percentage of replaced content of BAS (=percentage of BAS's weight to total sand weight);  $R_{BAC}$  is the percentage of replaced content of BAC (=percentage of BAC's weight to total coarse weight);  $\rho_c$  is the oven-dried density (in  $\text{kg/m}^3$ ), which can be obtained from Eq. 3;  $\rho_0$  is the reference

density (2300 kg/m<sup>3</sup>); and  $C/W$  is the cement-to-water ratio.

Values of  $f'_{c,meas}$  were also affected by  $R_{BAS}$ ,  $R_{BAC}$ , and  $W/C$ , wherein  $R_{BAS}$  and  $R_{BAC}$  are related to  $\rho_{c,meas}$ .  $\alpha_2$  in Eq. 5 was derived by first determining the relationship between  $R_{BAC}$  and  $f'_{c,meas}$  and then determining the relationship between  $W/C$  and  $f'_{c,meas}$ .  $\beta_2$  in Eq. 6 was also derived by first determining the relationship between  $R_{BAS}$  and  $f'_{c,meas}$ . Following that, the relationship between  $W/C$  and  $f'_{c,meas}$  was discerned. For NLR analysis, Fig. 3 shows the relationship between  $f'_{c,meas}$  and the fundamental form with  $C/W$  and  $\rho_{c,meas}$  multiplied by the coefficient factors, where all individually measured values were used, not the average values from Table 1.

Fig. 4 displays the comparison between  $f'_{c,meas}$  and predicted compressive strength ( $f'_{c,pred}$ ) using the proposed equations (Eqs. (4)–(6)) and Lee et al.'s (2019a) equation, where  $f'_{c,pred}$  was calculated with the predicted oven-dried density obtained from Eq. 3. Values of  $\gamma_m$ ,  $\gamma_{sd}$ , and  $\gamma_{cv}$  of LWAC-BA obtained by using the proposed equation are 1.03, 0.03, and 0.12, respectively. Meanwhile, values of  $\gamma_m$ ,  $\gamma_{sd}$ , and  $\gamma_{cv}$  of LWAC-BA within Lee et al.'s (2019a) equation are 1.29, 0.22, and 0.17, respectively. Overall, the proposed equation offers better accuracy than Lee et al.'s equation.

### 2.3 Elastic Modulus

ACI-318 (2019), MC2010 (2010), and Lee et al.'s (2019a) equation for predicting the elastic modulus of concrete ( $E_c$ ) are formulated with  $f'_c$  and  $\rho_c$ ; the results indicate that  $E_c$  is significantly affected by  $f'_c$  and  $\rho_c$ . Following the analysis method conducted by Lee et al. (2019a), the relationship between  $f'_{c,meas}\rho_{c,meas}/\rho_0$  and the measured elastic modulus ( $E_{c,meas}$ ) of LWAC-BA was studied, as shown in Fig. 5. The value of  $E_{c,meas}$  increased as  $f'_{c,meas}$  and/or  $\rho_{c,meas}$  increased. From the NLR analysis based

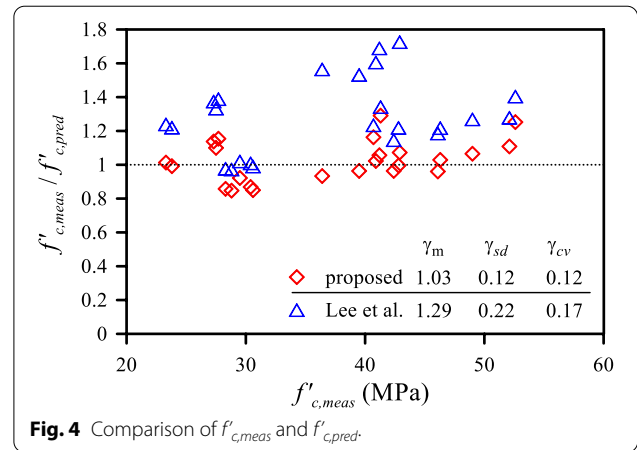


Fig. 4 Comparison of  $f'_{c,meas}$  and  $f'_{c,pred}$

on the test results, the elastic modulus  $E_c$  (in MPa) of LWAC-BA can be expressed using  $f'_c$  and  $\rho_c$  as

$$E_c = 7307 \left[ f'_c \left( \frac{\rho_c}{\rho_0} \right) \right]^{0.336}, \quad (7)$$

where  $f'_c$  is the compressive strength (in MPa), which can be obtained from Eq. 4;  $\rho_c$  is the oven-dried density (in kg/m<sup>3</sup>), which can be obtained from Eq. 3; and  $\rho_0$  is the reference density (2300 kg/m<sup>3</sup>).

Fig. 6 compares  $E_{c,meas}$  to the predicted concrete modulus ( $E_{c,pred}$ ) calculated with the predicted concrete strength and oven-dried density. As observed in Eq. 7 and other existing equations, the values of  $\gamma_m$ ,  $\gamma_{sd}$ , and  $\gamma_{cv}$  of LWAC-BA obtained by using the proposed equation are 1.00, 0.05, and 0.05, respectively, indicating that the proposed equation is excellent in terms of all indexes. The accuracy of the equation of Lee et al. (2019a) is good when  $E_{c,meas}$  is greater than 22,000 MPa. Meanwhile, the accuracy of MC2010 (2010) is good when  $E_{c,meas}$  is less than 22,000 MPa.

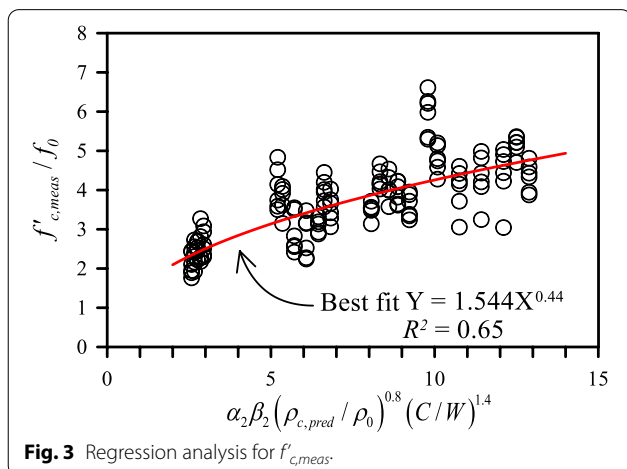


Fig. 3 Regression analysis for  $f'_{c,meas}$

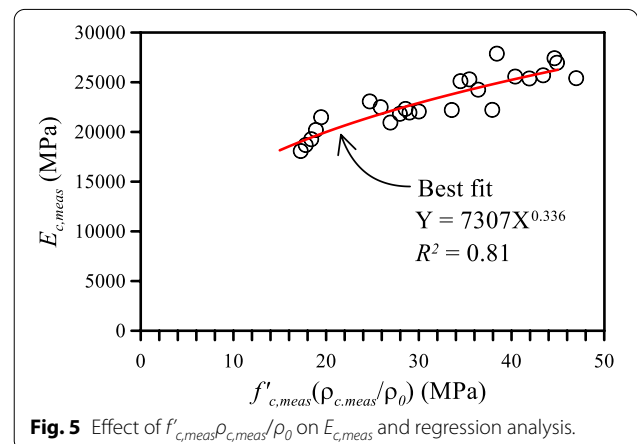
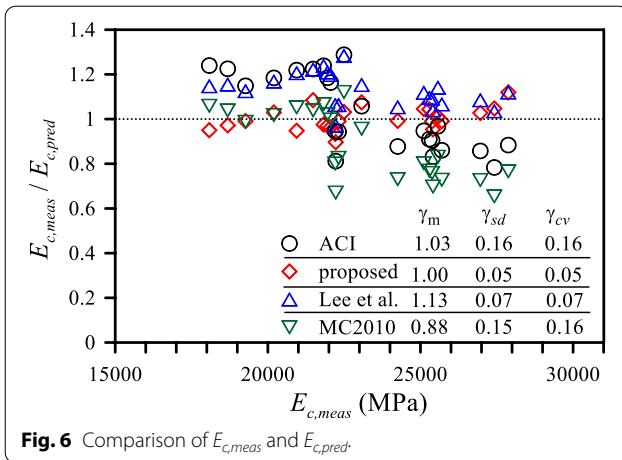
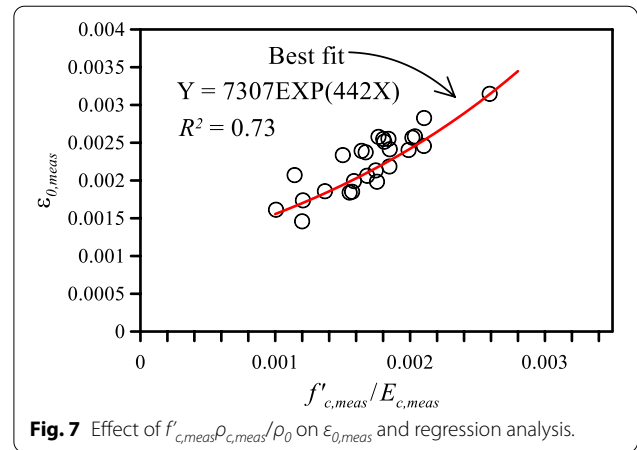


Fig. 5 Effect of  $f'_{c,meas}\rho_{c,meas}/\rho_0$  on  $E_{c,meas}$  and regression analysis.



**Fig. 6** Comparison of  $E_{c,meas}$  and  $E_{c,pred}$



**Fig. 7** Effect of  $f'_{c,meas} \rho_{c,meas} / \rho_0$  on  $\epsilon_{0,meas}$  and regression analysis.

### 2.4 Stress–Strain Relationship

Yang et al. (2014a, 2014b) proposed an equation for predicting the stress–strain curve of concrete, including the descending branch covering a wide range of  $f'_c$  values (from 10 to 180 MPa) and  $\rho_c$  values (from 1200 to 4500 kg/m<sup>3</sup>). Further, Lee et al. (2019a) presented a modified equation for LWAC-BS by performing the same analysis as that of Yang et al. (2014a, 2014b) with the test database of LWAC-BS. The two equations have the same fundamental equation (Eq. 8) regarding the corresponding concrete stress ( $f'_{c,crs}$ ) and specific strain ( $\epsilon_c$ ), as well as the equation related to ascending and descending branches being different depending on the properties of the concrete:

$$f'_{c,crs} = \left[ \frac{(\beta + 1) \left( \frac{\epsilon_c}{\epsilon_0} \right)}{\left( \frac{\epsilon_c}{\epsilon_0} \right)^{\beta+1} + \beta} \right] f'_c, \tag{8}$$

where  $f'_{c,crs}$  is the corresponding concrete stress (in MPa) for the specific strain ( $\epsilon_c$ );  $\epsilon_0$  is the strain value at peak stress;  $f'_c$  is the compressive strength (in MPa) of LWAC-BA, respectively; and  $\beta$  is the key parameter determining slopes of the ascending and descending branches of the stress–strain curve.

Yang (2019, 2020) reported that it was difficult to measure a descending branch because of the brittle characteristic of LWAC-BA. Therefore, there are a few data points including a descending branch. For NLR analysis, the relationship of the measured specific strain ( $\epsilon_{0,meas}$ ) and  $f'_{c,meas} / E_{c,meas}$  was first studied, as shown in Fig. 7. Hence, the equation to predict  $\epsilon_0$  at the peak compressive strength of LWAC-BA can be expressed as:

$$\epsilon_0 = 0.001 \exp \left[ 442 \left( \frac{f'_c}{E_c} \right) \right]. \tag{9}$$

When entering Eq. 9 into Lee et al.’s (2019a) equation, it was found that the slopes of the ascending branch were close to the measured slope, although the slopes of the descending branch were different. Therefore, it was decided that only the equation of the descending branch should be modified, and the constant in the exponential function was changed from 0.58 to 0.3, with the slopes of the descending branch compared with the measured values (Fig. 8). Therefore, the equations for the ascending and descending branches can be expressed as

$$\beta = 0.19 \exp \left[ 0.54 \left( \frac{f'_c}{f_0} \right) \left( \frac{\rho_0}{\rho_c} \right)^{1.5} \right] \text{ for } \epsilon_c \leq \epsilon_0, \tag{10}$$

$$\beta = 0.32 \exp \left[ 0.3 \left( \frac{f'_c}{f_0} \right) \left( \frac{\rho_0}{\rho_c} \right)^{1.5} \right] \text{ for } \epsilon_c > \epsilon_0. \tag{11}$$

$f'_c$  and  $\rho_c$  are the compressive strength (in MPa) and oven-dried density (in kg/m<sup>3</sup>) of LWAC-BA, respectively; and  $f_0$  and  $\rho_0$  are the 10 MPa and 2300 kg/m<sup>3</sup> reference values. Equation 10 is the same equation proposed by Lee et al. (2019a).

Fig. 9 displays the ratios of the measured strain ( $\epsilon_{0,meas}$ ) to predicted strain ( $\epsilon_{0,pred}$ ) at peak compressive strength, where values of  $\epsilon_{0,pred}$  are calculated with the predicted compressive strength ( $f'_{c,pred}$ ) and elastic modulus ( $E_{c,pred}$ ) of LWAC-BA. All indexes of the proposed equation for reliability are excellent in the overall range. The accuracy

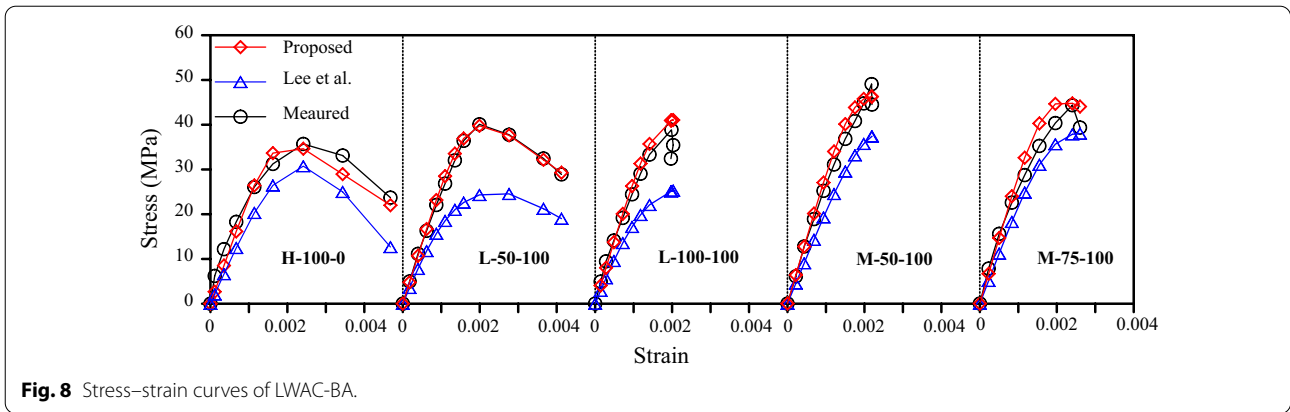


**Fig. 8** Stress–strain curves of LWAC-BA.

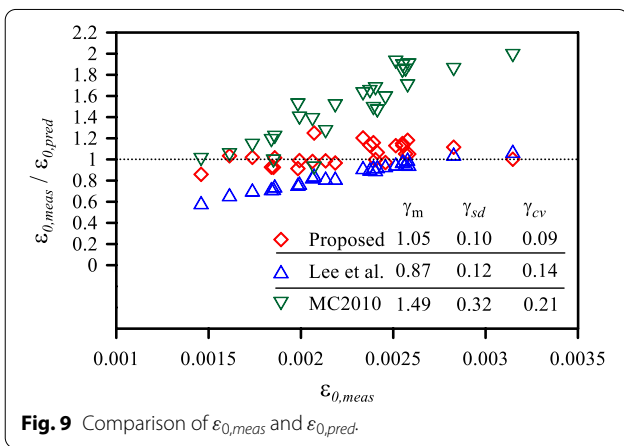


**Fig. 9** Comparison of  $\epsilon_{0,meas}$  and  $\epsilon_{0,pred}$ .

of Lee et al.'s (2019a) equation increases as the value of  $\epsilon_{0,meas}$  increases.

### 2.5 Splitting Tensile Strength, Modulus of Rupture, and Bond Strength

Lee et al. (2019a) also proposed the splitting tensile strength ( $f_{sp}$ ), modulus of rupture ( $f_r$ ), and bond strength ( $\tau_b$ ) based on  $f'_c$  and  $\rho_c/\rho_0$ , and the design equations were expressed through the form of  $\{(f'_c)^{n_1} (\rho_c/\rho_0)^{n_2}\}^\alpha$ , where  $n_1$ ,  $n_2$ , and  $\alpha$  as three exponents are the coefficient factors that vary based on mechanical properties. This means that  $f_{sp}$ ,  $f_r$ , and  $\tau_b$  are strongly affected by  $f'_c$  and  $\rho_c$ , and the relation of  $f_{sp}$ ,  $f_r$ , and  $\tau_b$  and  $\{(f'_c)^{n_1} (\rho_c/\rho_0)^{n_2}\}^\alpha$  was also investigated in this study.

Fig. 10 shows the effects of  $f'_{c,pred}\rho_{c,pred}/\rho_0$  on the measured splitting tensile strength ( $f_{sp,meas}$ ), measured modulus of rupture ( $f_{r,meas}$ ), and measured bond strength ( $\tau_{b,meas}$ ) of LWAC-BA, where  $\rho_{c,pred}$  and  $f'_{c,pred}$  are the predicted density and compressive strength obtained from Eqs. 3 and 4, respectively. The values of  $f_{sp,meas}$ ,  $f_{r,meas}$ , and  $\tau_{b,meas}$  of LWAC-BA increased with the rise in  $f'_{c,pred}$  and/

or  $\rho_{c,pred}$ . From the LNR analysis in Fig. 10,  $f_{sp}$ ,  $f_r$ , and  $\tau_b$  of LWAC-BA can be expressed using  $f'_c$  and  $\rho_c$  as:

$$f_{sp} = 0.5 \left( f'_c \left( \frac{\rho_c}{\rho_0} \right) \right)^{0.54}, \tag{12}$$

$$f_r = 1.74 \left( f'_c \left( \frac{\rho_c}{\rho_0} \right) \right)^{0.32}, \tag{13}$$

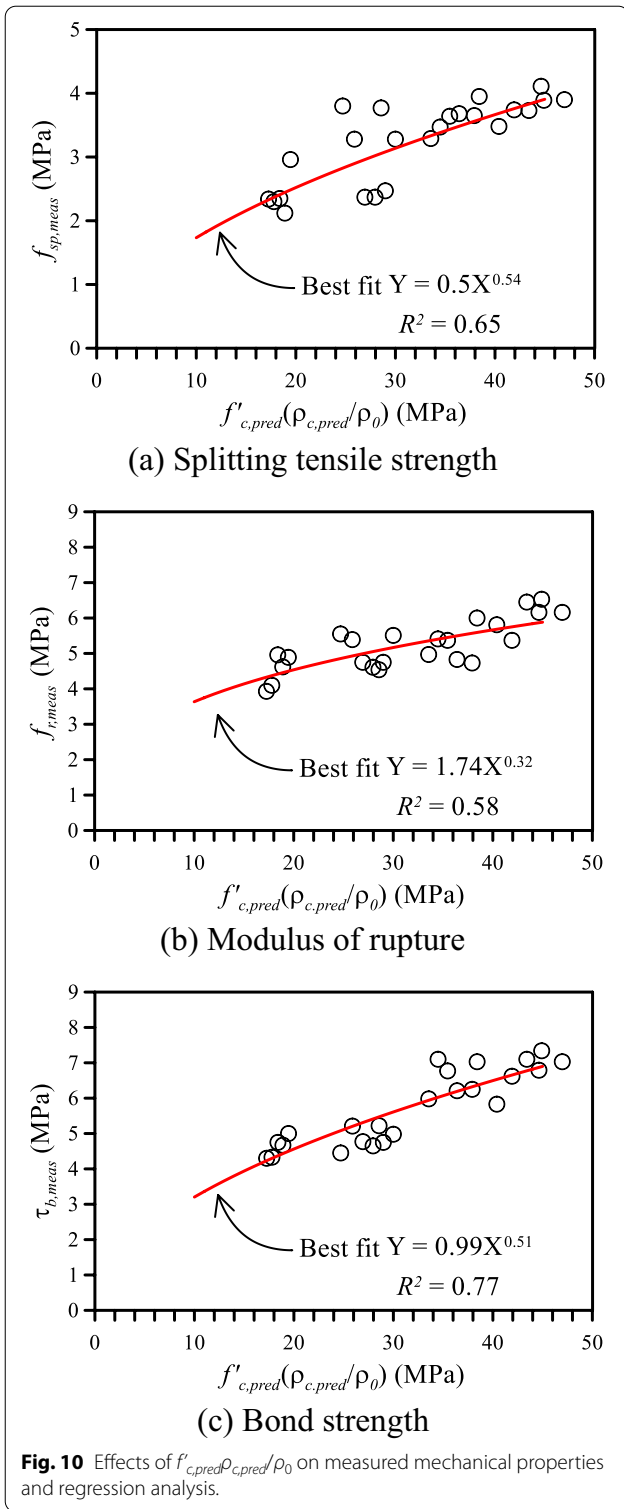
$$\tau_b = 0.99 \left( f'_c \left( \frac{\rho_c}{\rho_0} \right) \right)^{0.51}, \tag{14}$$

where  $f_{sp}$ ,  $f_r$ , and  $\tau_b$  are the predicted splitting tensile strength (in MPa), modulus of rupture (in MPa), and bond strength (in MPa), respectively;  $f'_c$  is the compressive strength (in MPa);  $\rho_c$  is the oven-dried density (in kg/m<sup>3</sup>); and  $\rho_0$  is the reference density (2300 kg/m<sup>3</sup>). Here,  $\rho_c$  and  $f'_c$  can be obtained from Eqs. 3 and 4.

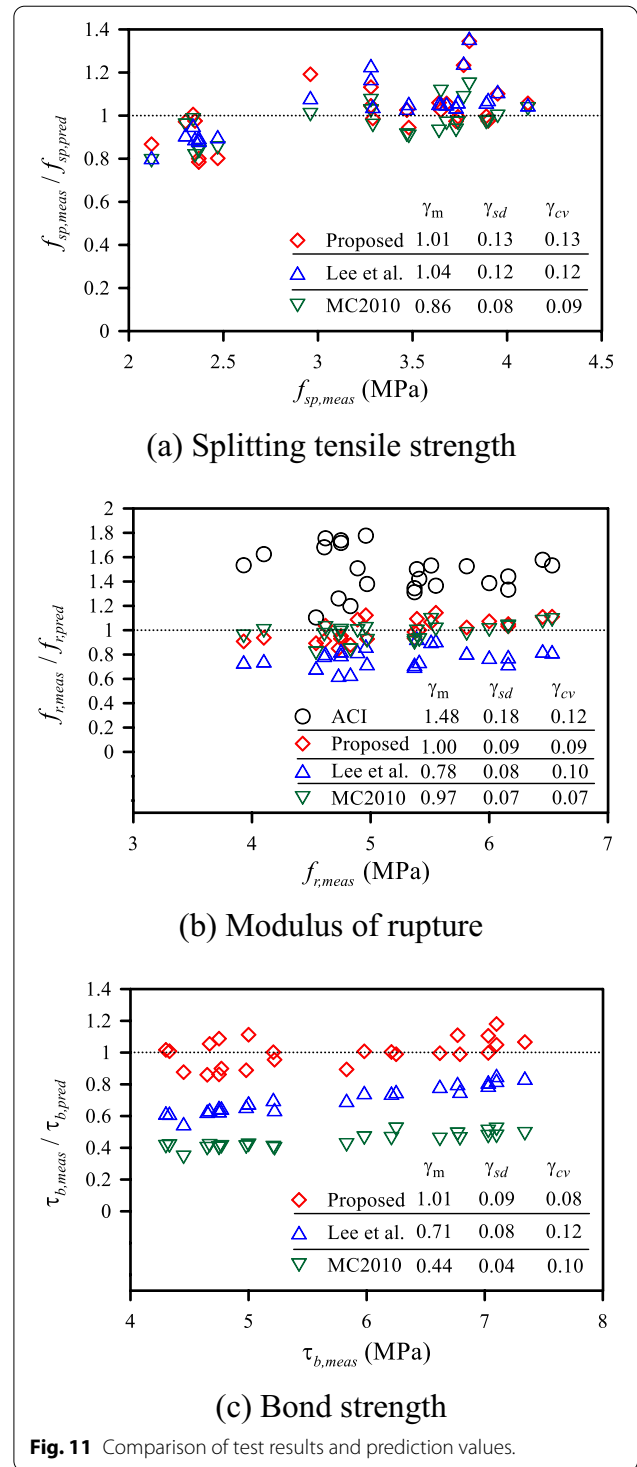
Fig. 11 presents a comparison of the test results and the predicted values iterated by the equation of Lee et al (2019a), ACI-318 (2019), MC 2010 (2010), and the proposed equation. All equations overestimate  $f_{sp}$  in  $f_{sp,meas}$  range of 2.5 MPa or less, and they exhibit solid accuracy in  $f_{sp,meas}$  range of 3 MPa or greater. In the case of  $f_r$ , the values of  $\gamma_m$  of the proposed equation and MC2010 (2010) are close to 1.0, while the equation of ACI-318 (2019) underestimates across the entire range. Regarding  $\tau_b$ , the values of  $\gamma_m$  and  $\gamma_{cv}$  of LWAC-BA obtained using the proposed equation are 1.01 and 0.08, respectively, which are the best values among all the equations.

### 3 Conclusions

In this study, empirical equations were derived from the experimental results for oven-dried density ( $\rho_c$ ), compressive strength ( $f'_c$ ), splitting strength ( $f_{sp}$ ), bond strength ( $\tau_b$ ), elastic modulus ( $E_c$ ), and stress–strain curve of lightweight concrete made with bottom ash fine



and/or coarse aggregates, which was suitable material for lightweight aggregate concrete because of its low density. The following conclusions could be made:



1. The density and compressive strength were comprehensively affected by the combination of the water-to-cement ( $W/C$ ) ratio and replacement ratios of bottom ash fine and/or coarse aggregates. The proposed

equations for density and compressive strength include coefficient factors that consider their effects, where one coefficient factor is considered with  $W/C$  and the replaced content ratio of bottom ash fine aggregate ( $R_{BAS}$ ) and the other is considered with  $W/C$  and the replaced content ratio of bottom ash coarse aggregate ( $R_{BAC}$ ). In particular, the oven-dried density is a key parameter for determining the lightweight aggregate concrete made with bottom ash aggregate (LWAC-BA), affecting compressive strength, elastic modulus, stress–strain curve, splitting tensile strength, modulus of rupture, and bond strength.

2. Straightforward empirical equations are derived from experimental data and NLR analysis to predict the mechanical properties of LWAC-BA. The values of the mean ( $\gamma_m$ ), standard deviation ( $\gamma_{sd}$ ), and coefficient of variation ( $\gamma_{cv}$ ) of the ratios between experiments and predictions of the mechanical properties of LWAC-BA range from 1.00 to 1.05, from 0.02 to 0.013, and from 0.02 to 0.13, respectively. Overall, the proposed equations are in good agreement with the experimental results.
3. In this study, the proposed empirical equation for the stress–strain relationship is developed for LWAC-BA and is compared to the equation proposed by Lee et al. (2019a). The equation of Lee et al. (2019a) and the proposed equation are in good agreement with the ascending branches, but the proposed equation is only fit to the descending branch.
4. ACI-318 (2019) underestimates the modulus of rupture of LWAC-BA; MC2010 (2010) overestimates the bond strength and splitting tensile strength of LWAC-BA but underestimates the strain corresponded with peak compressive strength. As the existing models and codes are not considered with bottom ash aggregate, the accuracy for LWAC-BA is relatively lower than that of the proposed empirical equation in this study.

#### Acknowledgements

This research was supported by Korea South-East Power Co. and the Korea Agency for Infrastructure Technology Advancement (KAIA) grant funded by the Ministry of Land, Infrastructure and Transport (Grant 22NANO-C156177-03).

#### Authors' contributions

All the authors contributed to this research with respect to the following: the first and second authors analyzed the data and wrote the paper; the second and third authors derived the mathematical model; and the fourth and fifth authors reviewed the previous relevant research and code provisions. All authors read and approved the final manuscript.

#### Authors' information

Hye-Jin Lee, Ph.D candidate, Department of Architectural Engineering, Kyonggi University, Suwon, Kyonggi-Do, 16227, Republic of Korea. Sanghee

Kim, Assistant Professor, Department of Architectural Engineering, Kyonggi University, Suwon, Kyonggi-Do, 16227, Republic of Korea. Hak-Young Kim, Research Professor, Department of Architectural Engineering, Kyonggi University, Suwon, Kyonggi-Do, 16227, Republic of Korea. Ju-Hyun Mun, Assistant Professor, Department of Architectural Engineering, Kyonggi University, Suwon, Kyonggi-Do, 16227, Republic of Korea. Keun-Hyeok Yang, Professor, Department of Architectural Engineering, Kyonggi University, Suwon, Kyonggi-Do, 16227, Republic of Korea.

#### Funding

This study is funded by Korea South-East Power Co., Korea Agency for Infrastructure Technology Advancement, Grant 22NANO-C156177-03, Keun-Hyeok Yang.

#### Availability of data and materials

Not applicable.

#### Declarations

#### Competing interests

None of the authors have any competing interests in the manuscript.

Received: 18 April 2021 Accepted: 23 February 2022

Published: 3 May 2022

#### References

- ACI Committee 318. (2019). *Building Code Requirements for Structural Concrete (ACI 318–19)*. American Concrete Institute.
- Ferraro, C. C., Power, J. P., Roessler, J., Paris, J., & Townsend, T. G. (2016). From trash to treasure-pilot project demonstrates the potential for using waste-to-energy bottom ash as partial aggregate replacement in concrete pavement. *Concrete International*, 38(11), 46–51.
- fib. (2010). *Fédération Internationale du Béton*. (MC2010), The fib Model Code for Concrete Structures.
- Kim, H. K. (2015). Properties of normal-strength mortar containing coarsely - crushed bottom ash considering standard particle size distribution of fine aggregate. *Journal of the Korea Concrete Institute*, 27(5), 531–539. (in Korean).
- Kim, Y. H., Kim, H. Y., Yang, K. Y., & Ha, J. S. (2020). Evaluation of workability and mechanical properties of bottom ash aggregate concrete. *Applied Sciences*, 10(22), e8016.
- Kim, Y. H., Kim, H. Y., Yang, K. H., & Ha, J. S. (2021). Effect of concrete unit weight on the mechanical properties of bottom ash aggregate concrete. *Construction and Building Materials*, 273, e121998.
- Lee, K. H. (2018). Reliable model Proposals for Mechanical Properties and Mixing Proportioning of Lightweight Aggregate Concrete Using Expanded Bottom Ash and Dredged Soil Granules. Ph.D Dissertation. (in Korean)
- Lee, H. J., Kim, H. Y., & Yang, K. H. (2021). Compressive strength development model for bottom ash aggregates concrete. *Journal of the Korea Concrete Institute*, 33(4), 381–388. (in Korean).
- Lee, K. H., Yang, K. H., Mun, J. H., & Kwon, S. J. (2019a). Mechanical properties of concrete made from different expanded lightweight aggregates. *ACI Materials Journal*, 116(2), 9–19.
- Lee, K. H., Yang, K. H., Mun, J. H., & Tuan, N. V. (2019b). Effect of sand content on the workability and mechanical properties of concrete using bottom ash and dredged soil-based artificial lightweight aggregates. *International Journal of Concrete Structures and Materials*, 13(1), 115–127.
- Leiva, C., Vilches, L. F., Arenas, C., Delgado, S., & Fernandez-Pereira, C. (2012). Potential recycling of bottom and fly Ashes in acoustic mortars and concretes. *ACI Materials Journal*, 109(5), 529–535.
- Michaels, T., Shiang, I., (2016). Directory of waste-to-energy facilities, Energy Recovery Council.
- Nisnevich, M. (1997). Improving lightweight concrete with bottom ash. *Concrete International*, 19(12), 56–60.
- Nisnevich, M., Schlesinger, T., Eshel, Y., & Grof, Y. (1999). Lightweight concrete with bottom ash-radiological aspects. *ACI Materials Journal*, 96(2), 250–254.

- Sim, J. I., & Yang, K. H. (2011). Structural safety of lightweight aggregate concrete. *Journal of the Korea Concrete Institute*, 23(5), 27–32. (in Korean).
- Yang, K. H. (2019). Evaluation of mechanical properties of lightweight concrete using bottom ash aggregates. *Journal of the Korea Concrete Institute*, 31(4), 331–337. (in Korean).
- Yang, K. H. (2020). Development of replacement technology for ready mixed concrete with bottom ash aggregates, Report, Kyonggi University, (in Korean)
- Yang, K. H., Hwang, Y. H., Lee, Y., & Mun, J. H. (2019). Feasibility test and evaluation models to develop sustainable insulation concrete using foam and bottom ash aggregates. *Construction and Building Materials*, 225, 620–632.
- Yang, K. H., Kim, G. H., & Choi, Y. H. (2014a). An initial trial mixture proportioning procedure for structural lightweight aggregate concrete. *Construction and Building Materials*, 55, 431–439.
- Yang, K. H., Mun, J. H., Cho, M. S., & Kang, T. H. (2014b). A stress-strain model for various unconfined concrete in compression. *ACI Structural Journal*, 111(4), 819–826.
- Zang, B., & Poon, C. S. (2015). Use of furnace bottom ash for producing lightweight aggregate concrete with thermal insulation properties. *Journal of Cleaner Production*, 99, 94–100.

### Publisher's Note

Springer Nature remains neutral with regard to jurisdictional claims in published maps and institutional affiliations.

Submit your manuscript to a SpringerOpen<sup>®</sup> journal and benefit from:

- ▶ Convenient online submission
- ▶ Rigorous peer review
- ▶ Open access: articles freely available online
- ▶ High visibility within the field
- ▶ Retaining the copyright to your article

---

Submit your next manuscript at ▶ [springeropen.com](https://www.springeropen.com)

---